Published in final edited form as:
IEEE Trans Biomed Eng. 2010 March ; 57(3): 616–625. doi:10.1109/TBME.2009.2032533.

A Spatio-Temporal Framework for MEG/EEG Evoked Response Amplitude and Latency Variability Estimation

Tulaya Limpiti [Member, IEEE],
Faculty of Engineering, King Mongkut's Institute of Technology Ladkrabang, Bangkok 10520, Thailand.

Barry D. Van Veen [Fellow, IEEE], and
Department of Electrical and Computer Engineering, University of Wisconsin-Madison, 1415 Engineering Drive, Madison, WI 53706 USA.

Ronald T. Wakai
Department of Medical Physics, University of Wisconsin-Madison, WI 53706 USA.

Tulaya Limpiti: kltulaya@kmitl.ac.th; Barry D. Van Veen: vanveen@engr.wisc.edu; Ronald T. Wakai: rtwakai@facstaff.wisc.edu

Abstract

This paper presents a spatio-temporal framework for estimating single-trial response latencies and amplitudes from evoked response MEG/EEG data. Spatial and temporal bases are employed to capture the aspects of the evoked response that are consistent across trials. Trial amplitudes are assumed independent but have the same underlying normal distribution with unknown mean and variance. The trial latency is assumed to be deterministic but unknown. We assume the noise is spatially correlated with unknown covariance matrix. We introduce a generalized expectation-maximization algorithm called *TriViAL* (Trial Variability in Amplitude and Latency) which computes the maximum likelihood (ML) estimates of the amplitudes, latencies, basis coefficients, and noise covariance matrix. The proposed approach also performs ML source localization by scanning the TriViAL algorithm over spatial bases corresponding to different locations on the cortical surface. Source locations are identified as the locations corresponding to large likelihood values.

The effectiveness of the TriViAL algorithm is demonstrated using simulated data and human evoked response experiments. The localization performance is validated using tactile stimulation of the finger. The efficacy of the algorithm in estimating latency variability is shown using the known dependence of the M100 auditory response latency to stimulus tone frequency. We also demonstrate that estimation of response amplitude is improved when latency is included in the signal model.

Index Terms

Amplitude and/or latency variability; Evoked-response MEG/EEG; Expectation-maximization; Independent response; Maximum likelihood

I. INTRODUCTION

The underlying mechanisms for sensory perception and cognitive brain processes may be related to information encoded in measurable attributes of brain responses such as amplitude, latency, waveform morphology, or spatial and temporal patterns associated with particular events/tasks [1]–[7]. Magnetoencephalography and electroencephalography (MEG/EEG) are attractive tools for study of brain activity because they are non-invasive and have high temporal resolution suitable for tracking dynamic neural activity. Nevertheless, reliably estimating even

simple quantities such as amplitude or latency of a given response is a challenging task in MEG/EEG because of the low signal-to-noise ratio (SNR) typical of the recorded data. The blurring and mixing of cortical signals observed at the scalp further complicate response interpretation. Stimulus-locked averaging of evoked responses has long been employed to improve the SNR. Averaging can result in loss of amplitude and distortion of the estimated response waveform in the presence of latency jitter, such as is common with weak stimuli or late components [8], [9]. Furthermore, potentially useful information contained in trial-to-trial variations is not available from analysis of averaged data.

This paper presents a full spatio-temporal framework for estimating single-trial response latencies and amplitudes. Spatial and temporal bases are employed to capture the aspects of the evoked response that are consistent across trials. The spatial bases require that the signal originate from a specific location on the cortical surface or lie in a given subspace, while the temporal bases control attributes such as signal bandwidth, duration, or shape. Exploiting the spatio-temporal character of the evoked response results in improved estimates of latencies and amplitudes at realistic SNRs. The amplitudes are assumed independent between trials and are drawn from the identical underlying normal distribution with unknown mean and variance. The trial latency is assumed to be deterministic but unknown. We assume the noise is spatially correlated with unknown covariance matrix. Maximum likelihood (ML) estimates of the amplitudes, latencies, basis coefficients, and noise covariance matrix are obtained using a generalized expectation-maximization (EM) algorithm. We refer to this algorithm using the acronym *TriViAL* (Trial Variability in Amplitude and Latency). A key attribute of the proposed approach is the ability to perform ML source localization and response parameter estimation simultaneously. Source localization is performed by scanning the TriViAL algorithm over spatial bases corresponding to different locations on the cortical surface. Source locations are identified as the locations corresponding to large likelihood values. ML estimates of the signal waveform shape, noise covariance matrix, trial amplitudes, and trial latencies are then obtained using the spatial bases for the identified locations.

The effectiveness of the TriViAL algorithm is demonstrated using simulated data and two well-characterized evoked response experiments. The localization performance is validated using tactile stimulation of the finger, which is known to produce activity in the somatosensory areas of the cortex. The efficacy of the TriViAL algorithm in estimating latency variability is shown by corroborating the latency estimates with the known dependence of the auditory M100 response peak latency in MEG to the stimulus tone frequency [3], [10]. We also demonstrate that estimation of response amplitude is improved when latency is included in the signal model.

The TriViAL algorithm is an extension of our previously proposed generalized EM algorithm for estimating trial amplitude variability assuming latency is constant [11]. Both of these extend the constant response (CR) spatio-temporal ML approaches in [12]–[14] to estimate parameters of individual trials. A number of researchers have previously proposed algorithms for estimating amplitude and latency variability of individual trials, some of which are conceptually similar to the approach presented in this paper. The earliest work on estimating variable latencies is the ad hoc iterative scheme of Woody [15]. Woody proposes cross-correlating single-trial waveforms with a signal template, estimating latency based on the peak of the cross-correlation, then revising the template by averaging the individual waveforms after compensating for latency. Similar approaches based on maximal cross-correlation are reported in [6] and [16]. None of these employs a ML based spatio-temporal framework. ML approaches for estimating amplitude and latency variability include [9], [17], [18]. Both [9] and [17] unrealistically assume the background noise is spatially white and use only a single channel. De Munck, et al. [18] relax the uncorrelated background noise assumption and present a multichannel ML based approach for estimating trial amplitudes, spatiotemporal response waveform, and the spatial and temporal covariances of the noise. However, this method does

not relate the responses to cortical source space, does not estimate trial latencies and uses an ad hoc iterative algorithm that is not guaranteed to converge to ML estimates.

This paper is organized as follows. The following section presents the spatio-temporal signal model for the evoked response and the assumptions on the single-trial amplitudes and latencies. Development of the TriViAL algorithm for estimating latencies, amplitudes, and other response parameters is presented in Section III. Use of TriViAL for ML source localization is described in Section IV. Section V illustrates the effectiveness of the algorithm using simulated and real evoked response data. We conclude with a discussion in Section VI.

Bold upper and lower case symbols represent matrix and vector quantities, respectively. Superscripts T and −1 denote matrix transpose and inverse, respectively. The symbol tr {**A**} represents the trace of the matrix **A** and ⊗ denotes the Kronecker product. The operator vec {**A**} forms a vector from a matrix by stacking columns of **A**. The Frobenius norm of **A** is written as $\|\mathbf{A}\|_F$.

II. EVOKED RESPONSE SIGNAL MODEL

Assume the response amplitude and latency varies from trial to trial and the remaining spatio-temporal characteristics of the evoked response are constant across trials. We express the N by T matrix $\mathbf{S}_j$ representing the j^{th} trial of the response measured at N sensors and T time samples as

$$\mathbf{S}_j = \mathbf{U}(r)\mathbf{B}_j\mathbf{D}_j^T, \quad j=1,\ldots,J \tag{1}$$

where $\mathbf{U}(r)$ is the N by P known spatial basis matrix associated with location r on the cortical surface. Each of the P columns of $\mathbf{U}(r)$ is a basis vector; their linear combination gives rise to the observable spatial patterns at the N sensors. The L rows of the L by T_s matrix $\mathbf{C}^T$ are the known temporal bases, where we assume the response of interest exists over T_s time samples. Hence, The L by T trial-dependent temporal basis matrix $\mathbf{D}_j^T = \begin{bmatrix} 0\cdots 0 & \mathbf{C}^T & 0\cdots 0 \end{bmatrix}$ encodes the latency of the j^{th} trial, τ_j, as the number of zero columns that precedes the known temporal bases matrix $\mathbf{C}^T$. Here $\mathbf{B}_j$ is a $P \times L$ unknown basis coefficient matrix for the j^{th} trial and takes the form $\mathbf{B}_j = x_j\mathbf{B}$ where x_j is the amplitude of the trial and **B** defines the shape of the spatio-temporal response. Consequently, the spatio-temporal evoked response that is consistent across all trials is described by the N by T_s matrix $\mathbf{S} = \mathbf{U}(r)\mathbf{B}\mathbf{C}^T$. The quantities x_j and τ_j capture the amplitude and latency variability across trials, respectively.

The spatial bases $\mathbf{U}(r)$ may be chosen to model dipoles [19], multipoles [20], [21], or cortical patches [14]. In cases where source localization is not necessary or possible, $\mathbf{U}(r) = \mathbf{U}$ may be chosen based on the data, e.g., using spatially derived principal components. The temporal bases represent temporal attributes such as bandwidth or expected morphology [12], [13], and can be chosen in many ways, including Fourier bases or wavelets. Without loss of generality, we assume orthogonal basis functions, $\mathbf{U}(r)^T\mathbf{U}(r) = \mathbf{I}_P$ and $\mathbf{C}^T\mathbf{C} = \mathbf{I}_L$, and normalize the basis coefficient matrix such that $\|\mathbf{B}\|_F = 1$. In the subsequent sections, the dependence of the spatial basis $\mathbf{U}(r)$ on location r is dropped for notational convenience when there is no need to distinguish between different locations.

We model the amplitude of each response x_j as a sequence of statistically independent Gaussian distributed random variables with unknown prior mean μ_x and variance σ_x^2, that is,

$$x_j \sim p(x_j) = \mathcal{N}(\mu_x, \sigma_x^2), \; j=1,\ldots,J \tag{2}$$

where $\mathcal{N}(\mu_x, \sigma_x^2)$ denotes the normal density. The latency of each response, τ_j, is assumed deterministic but unknown.

The $N \times T$ matrix $\mathbf{Y}_j$ denotes the measured response and is modeled as

$$\boldsymbol{Y}_j = \mathbf{S}_j + \mathbf{N}_j, \quad j = 1, \ldots, J \tag{3}$$

Here the $N \times T$ matrix $\mathbf{N}_j$ is zero-mean Gaussian noise with unknown positive-definite spatial covariance $\mathbf{R}_n$ and known temporal covariance $\mathbf{R}_t$. We assume $\mathbf{R}_t = \mathbf{I}$ without loss of generality since the data may be prewhitened by the known $\mathbf{R}_t$. Hence, we write $\mathbf{N}_j \sim \mathcal{N}(\mathbf{0}, \mathbf{I} \otimes \mathbf{R}_n)$ where $\mathbf{I} \otimes \mathbf{R}_n$ is the covariance matrix of vec $\{\mathbf{N}_j\}$. The noise is assumed to be independent and identically distributed across trials. If we let $Y = \{\mathbf{Y}_1, \mathbf{Y}_2, \ldots, \mathbf{Y}_J\}$ denote the collection of measured data and $X = \{x_1, x_2, \ldots, x_J\}$ the set of unknown trial amplitudes, we may write the probability density for Y conditioned on X as

$$p(Y|X) = \prod_{j=1}^{J} p(\boldsymbol{Y}_j | x_j) \tag{4}$$

where

$$p(\boldsymbol{Y}_j | x_j) = \mathcal{N}(x_j \mathbf{U}\mathbf{B}\mathbf{D}_j^T, \mathbf{I} \otimes \mathbf{R}_n). \tag{5}$$

The matrix $\mathbf{I} \otimes \mathbf{R}_n$ is the covariance matrix of vec$\{\mathbf{Y}_j\}$ given x_j. It is implicit that the latencies τ_j are given or known for this conditional distribution.

III. THE TRIVIAL ALGORITHM

The TriViAL algorithm employs the expectation-conditional maximization (ECM) method [22] to obtain solutions for the ML estimates of the individual trial amplitudes and latencies, spatio-temporal waveform, spatial noise covariance matrix, and the prior mean μ_x and variance σ_x^2. ECM is a variant of the conventional EM algorithm that simplifies estimation of coupled parameters by sequentially solving for them in the conditional maximization (CM−) step. ECM retains the favorable convergence properties of EM provided the sequential estimates increase the likelihood. We treat the unknown trial amplitudes as the so-called hidden data. We combine the observed data Y with the hidden data to form the complete data $\{Y,X\}$. Estimates of the trial amplitudes X are obtained in the expectation (E−) step and the remaining unknown parameters including the trial latencies, $\Theta = \{\mathbf{R}_n, \mathbf{B}, \mu_x, \sigma_x^2, \tau_j\}$, are estimated in the conditional maximization step. Assuming the response amplitudes are independent allows closed-form expressions for the posterior mean of the x_j, which are taken as the updated estimates of the trial amplitude, and closed-form equations for updating the parameters in the CM-step of the TriViAL algorithm.

The complete-data log likelihood, $l(Y,X)$, is written as

$$l(Y, X) = \log p(Y, X) \tag{6}$$

$$= \sum_{j=1}^{J} [\log p(\boldsymbol{Y_j}|x_j) + \log p(x_j)] \tag{7}$$

Using (2) and (5) we can express (7), ignoring additive constants, as

$$\begin{aligned} l(Y, X) \propto & \\ & \tfrac{JT}{2}\log|\mathbf{R}_n^{-1}| + \tfrac{J}{2}\log(1/\sigma_x^2) - \tfrac{1}{2\sigma_x^2}\sum_j (x_j - \mu_x)^2 \\ & - \tfrac{1}{2}\sum_j \mathrm{tr}\left\{(\boldsymbol{Y_j} - x_j\mathbf{UBD}_j^T)^T \mathbf{R}_n^{-1}(\boldsymbol{Y_j} - x_j\mathbf{UBD}_j^T)\right\}. \end{aligned} \tag{8}$$

A. The E-Step

The expectation step in the $(k + 1)^{\text{th}}$ iteration computes the expected complete-data log likelihood or the Q-function, $Q(\Theta|\Theta^{(k)})$, where $\Theta^{(k)}$ denotes the parameter estimates from the CM-step in the previous iteration. The expectation is taken with respect to the conditional distribution of the hidden data given the observed data and $\Theta^{(k)}$, $p(X|Y,\Theta^{(k)})$. That is,

$$\begin{aligned} Q\left(\Theta|\Theta^{(k)}\right) &= \int l(Y, X)\, p\left(X|Y, \Theta^{(k)}\right) dX \\ &= \mathbf{E}_{X|Y,\Theta^{(k)}}[\, l(Y, X)]. \end{aligned} \tag{9}$$

Substituting (8) into (9) yields

$$\begin{aligned} Q\left(\Theta|\Theta^{(k)}\right) \propto & \\ & \tfrac{JT}{2}\log|\mathbf{R}_n^{-1}| + \tfrac{J}{2}\log(1/\sigma_x^2) \\ & - \tfrac{1}{2\sigma_x^2}\sum_j (\mathbf{E}[\, x_j^2] - 2\mu_x \mathbf{E}[\, x_j] + \mu_x^2) \\ & - \tfrac{1}{2}\sum_j \mathrm{tr}\{\boldsymbol{Y_j}^T \mathbf{R}_n^{-1} \boldsymbol{Y_j}\} \\ & - \tfrac{1}{2}\sum_j \left(\mathbf{E}[\, x_j^2]\, \mathrm{tr}\left\{(\mathbf{UBD}_j^T)^T \mathbf{R}_n^{-1} \mathbf{UBD}_j^T\right\}\right) \\ & + \sum_j (\mathbf{E}[\, x_j]\, \mathrm{tr}\{\boldsymbol{Y_j}^T \mathbf{R}_n^{-1} \mathbf{UBD}_j^T\}) \end{aligned} \tag{10}$$

where $\mathbf{E}[\cdot]$ in (10) is short-hand for $\mathbf{E}_{X|Y,\Theta^{(k)}}[\cdot]$. The expectation is taken with respect to the posterior distribution $p(x_j \mid \mathbf{Y}_j, \Theta^{(k)})$ and is not to be confused with the prior mean $\mathbf{E}X[x_j] = \mu_x$.

The first and second conditional moments $E_{X|Y,\Theta^{(k)}}[x_j]$ and $E_{X|Y,\Theta^{(k)}}[x_j^2]$ required to evaluate $Q(\Theta|\Theta^{(k)})$ are obtained from the posterior distribution $p(x_j \mid \mathbf{Y}_j, \Theta^{(k)})$. Since x_j and $\mathbf{Y}_j$ are jointly Gaussian (see (8)) and $p(x_j)$ is a conjugate prior, this posterior distribution is also Gaussian according to the Gauss-Markov theorem [23]. That is,

$$p\left(x_j|Y, \Theta^{(k)}\right) = \mathcal{N}(\bar{x}_j, \gamma^{-1}). \tag{11}$$

So $E_{X|Y,\Theta^{(k)}}[x_j] = \bar{x}_j$ and $E_{X|Y,\Theta^{(k)}}\left[x_j^2\right] = \bar{x}_j^2 + \gamma^{-1}$ where

$$\gamma = \text{tr}\left\{(\mathbf{U}\mathbf{B}\mathbf{D}_j^T)^T \mathbf{R}_n^{-1}(\mathbf{U}\mathbf{B}\mathbf{D}_j^T)\right\} + \frac{1}{\sigma_x^2} \tag{12}$$

$$\bar{x}_j = \gamma^{-1}\left(\text{tr}\left\{(\mathbf{U}\mathbf{B}\mathbf{D}_j^T)^T \mathbf{R}_n^{-1}\mathbf{Y}_j\right\} + \frac{\mu_x}{\sigma_x^2}\right). \tag{13}$$

In these expressions, $\mathbf{B}$, $\mathbf{R}_n$, σ_x^2, μ_x are replaced by their current estimates $\mathbf{B}(k)$, $\mathbf{R}_n^{(k)}$, $\sigma_x^{2(k)}$, and $\mu_x^{(k)}$ from the preceding CM-step. Similarly, the position of $\mathbf{C}$ in $\mathbf{D}_j$ changes according to the current estimated latency $\tau_j^{(k)}$. The posterior mean $\bar{x}_j$'s are interpreted as estimates of the trial amplitude for the k-th iteration and have variance of γ^{-1}.

B. The CM-Step

The CM-step updates the value of the trial latency and the remaining parameters in Θ by maximizing $Q(\Theta|\Theta^{(k)})$ with respect to Θ. To help stabilize the noise covariance matrix estimate, we modify the ML cost function using an inverse Wishart prior as

$$\begin{aligned}\tilde{Q}\left(\Theta|\Theta^{(k)}\right) = \; & Q\left(\Theta|\Theta^{(k)}\right) + \tfrac{\rho}{2}\log|\mathbf{R}_n^{-1}| \\ & -\tfrac{1}{2}\text{tr}\{\Lambda\mathbf{R}_n^{-1}\}\end{aligned} \tag{14}$$

where $\log p(\mathbf{R}_n^{-1}) \propto \frac{\rho}{2}\log|\mathbf{R}_n^{-1}| - \frac{1}{2}\text{tr}\{\Lambda\mathbf{R}_n^{-1}\}$ is a Wishart prior on the inverse of the spatial noise covariance matrix and $\rho = 1$.

We partition the parameters into subsets $\Theta_1 = \{\mathbf{R}_n, \mu_x\}$, $\Theta_2 = \{\mathbf{B}, \sigma_x^2\}$, and $\Theta_3 = \{\tau_j\}$. The CM-step update involves sequentially solving a three-step maximization problem,

$$\begin{aligned}\Theta_1^{(k+1)} &= \arg\max_{\Theta_1}\left\{Q\left(\Theta|\Theta^{(k)}\right):\Theta_2=\Theta_2^{(k)}, \Theta_3=\Theta_3^{k}\right\} \\ \Theta_2^{(k+1)} &= \arg\max_{\Theta_2}\left\{Q\left(\Theta|\Theta^{(k)}\right):\Theta_1=\Theta_1^{(k+1)}, \Theta_3=\Theta_3^{(k)}\right\} \\ \Theta_3^{(k+1)} &= \arg\max_{\Theta_3}\left\{Q\left(\Theta|\Theta^{(k)}\right):\Theta_1=\Theta_1^{(k+1)}, \Theta_2=\Theta_2^{(k+1)}\right\}\end{aligned}$$

The likelihood is always increased in each substep, and so the CM-step monotonically increases the likelihood at each iteration and convergence of the ECM algorithm to a local maximum is guaranteed.

The update equations for the new parameter estimates $\Theta^{(k+1)}$ are obtained by setting the derivative of $Q(\Theta|\Theta^{(k)})$ with respect to each parameter of interest to zero. Maximizing $\tilde{Q}(\Theta|\Theta^{(k)})$ with respect to $\Theta_1 = \{\mathbf{R}_n, \mu_x\}$ gives

$$\begin{aligned}\mathbf{R}_n^{(k+1)} = \; & \tfrac{1}{JT+\rho}\Big[\mathbf{R}_{yy} - \mathbf{U}\mathbf{B}^{(k)}\mathbf{R}_{xy}^T \\ & -\mathbf{R}_{xy}\left(\mathbf{U}\mathbf{B}^{(k)}\right)^T + \Lambda \\ & + \left(\mathbf{U}\mathbf{B}^{(k)}\right) R_{xx}\left(\mathbf{U}\mathbf{B}^{(k)}\right)^T\Big]\end{aligned} \tag{15}$$

$$\mu_x^{(k+1)} = \frac{1}{J}\sum_j \bar{x}_j \tag{16}$$

where

$$\mathbf{R}_{yy} = \sum_j \boldsymbol{Y}_j \boldsymbol{Y}_j^T \tag{17}$$

$$\mathbf{R}_{xy} = \sum_j \bar{x}_j \boldsymbol{Y}_j \mathbf{D}_j \tag{18}$$

$$R_{xx} = \sum_j (\bar{x}_j^2) + J\gamma^{-1}. \tag{19}$$

Note that the dependence of $\bar{x}_j$, γ, $\mathbf{R}_{xy}$, and R_{xx} on the iteration k is suppressed for notational convenience. Next we maximize with respect to $\Theta_2 = \{\mathbf{B}, \sigma_x^2\}$ to obtain

$$\mathbf{B}^{(k+1)} = \left[R_{xx}\mathbf{U}^T \left(\mathbf{R}_n^{(k+1)}\right)^{-1} \mathbf{U}\right]^{-1} \times \mathbf{U}^T \left(\mathbf{R}_n^{(k+1)}\right)^{-1} \mathbf{R}_{xy} \tag{20}$$

$$\sigma_x^{2(k+1)} = \left(\frac{1}{J}\sum_j \bar{x}_j^2\right) + \gamma^{-1} - \left(\mu_x^{(k+1)}\right)^2. \tag{21}$$

The final substep updates the estimates of latencies $\{\tau_j\}$. Because of the independence between trials, each latency τ_j is estimated independently. The only term in $Q(\Theta|\Theta^{(k)})$ that is dependent on τ_j is

$$Q\left(\Theta|\Theta^{(k)}\right) \propto \bar{x}_j \mathrm{tr}\left\{\boldsymbol{Y}_j^T \mathbf{R}_n^{-1} \mathbf{U}\mathbf{B}\mathbf{D}_j^T\right\} \tag{22}$$

Hence,

$$\tau_j^{(k+1)} = \max_{\tau_j} \mathrm{tr}\left\{\boldsymbol{Y}_j^T \left(\mathbf{R}_n^{(k+1)^{-1}}\right) \mathbf{U}\mathbf{B}^{(k+1)}\mathbf{D}_j^T\right\} \tag{23}$$

That is, the latency estimate is given as the time point at which the correlation between the current estimate of the whitened signal $\left(\mathbf{R}_n^{(k+1)}\right)^{-1/2}\mathbf{U}\mathbf{B}^{(k+1)}\mathbf{C}^T$ and the whitened data $\left(\mathbf{R}_n^{(k+1)}\right)^{-1/2}\boldsymbol{Y}_j$ is greatest.

In practice, we discretize the search space for τ_j to integer multiples of the sampling interval and perform exhaustive search of the best τ_j in a physically feasible range. This discretization avoids the complication of accounting for changes in response morphology associated with fractional delays. In practice MEG/EEG is typically over-sampled and thus the latency quantum is much smaller than the inverse of the response bandwidth. If finer precision is needed than that provided by the sampling interval, the data can be interpolated to decrease the sampling interval prior to processing. Note that noise and trial to trial variations in waveform shape limit the practical utility of very fine scale latency estimates.

The TriViAL algorithm iterates between updating the amplitude estimates in the E-step and the latency estimates and other parameters in the CM-step until the original data log likelihood $l(Y)$ converges to a local maximum. The data log likelihood used to terminate the algorithm is

$$\begin{aligned} l(Y)^{(k)} = & \\ & -\tfrac{JT+\rho}{2}\log\left|\mathbf{R}_n^{(k)}\right| - \tfrac{1}{2}\mathrm{tr}\left\{\mathbf{\Lambda}\mathbf{R}_n^{(k)^{-1}}\right\} \\ & -\tfrac{J}{2}\log\left(1+\sigma_x^{2(k)}\,\mathrm{tr}\left\{\mathbf{B}^{(k)^T}\mathbf{U}^T\mathbf{R}_n^{(k)^{-1}}\mathbf{U}\mathbf{B}^{(k)}\right\}\right) \\ & -\tfrac{1}{2}\sum_j\left[\mathrm{tr}\left\{\tilde{\mathbf{G}}_j^T\mathbf{R}_n^{(k)^{-1}}\tilde{\mathbf{G}}_j\right\}\right] \\ & +\tfrac{1}{2}\sum_j\left[\tilde{\alpha}\left(\mathrm{tr}\left\{\tilde{\mathbf{G}}_j^T\mathbf{R}_n^{(k)^{-1}}\mathbf{U}\mathbf{B}^{(k)}\mathbf{D}_j^T\right\}\right)^2\right] \end{aligned} \tag{24}$$

where $\tilde{\mathbf{G}}_j = \boldsymbol{Y}_j - \mu_x^{(k)}\mathbf{U}\mathbf{B}^{(k)}\mathbf{D}_j^T$ and $\tilde{\alpha} = \left[\frac{1}{\sigma_x^{2(k)}} + \mathrm{tr}\left\{\mathbf{B}^{(k)^T}\mathbf{U}^T\mathbf{R}_n^{(k)^{-1}}\mathbf{U}\mathbf{B}^{(k)}\right\}\right]^{-1}$. Let $\left\{\widehat{\mathbf{R}}_n, \widehat{\sigma}_x^2, \widehat{\mathbf{B}}, \widehat{\mu}_x\right\}$ be the parameter estimates after convergence of $l(Y)$. The spatio-temporal evoked response shape estimate is $\mathbf{S}^{\wedge} = \mathbf{U}\hat{\mathbf{B}}\mathbf{C}^T$.

IV. SOURCE LOCALIZATION USING TRIVIAL

Recall that the spatial bases $\mathbf{U}(r)$ relate the activity at cortical location r to the measured data. The TriViAL algorithm can be used for ML source localization by scanning the likelihood $l(Y)$ over different locations r on the surface using the spatial bases $\mathbf{U}(r)$. This results in a log likelihood value $l(Y; \mathbf{U}(r))$ that is an explicit function of location. The ML estimate of r is the value that maximizes $l(Y; \mathbf{U}(r))$.

V. RESULTS

Real and simulated evoked response data are used to illustrate the effectiveness of the algorithm in localizing neural activity and estimating trial-to-trial amplitude and latency variability. In examples where localization is illustrated, dipolar leadfield matrices are used as the spatial bases for both localization and estimation. These are calculated for the $N = 74$ channels Magnes II Biomagnetometer system (Biomagnetic Technologies, Inc.) assuming a dual sphere forward model. In the remaining examples, source localization is not performed and two dominant principal components derived from the filtered and averaged data are used as spatial bases for signal estimation.

A. Simulated Data

We simulate focal neural activity by placing a single dipolar source in the somatosensory area and generate 300 trials of evoked response recordings. The signal duration is 53.76 ms or $T_s = 28$ time samples at 520.8 Hz sampling rate. The signal waveform has a raised cosine shape

with 17.5 ms full width at half maximum (FWHM) as shown in Fig. 1(a). The observation interval is 107.52 ms or $T = 56$ time samples in length. The simulated response amplitudes are chosen to have an initial habituation effect followed by an oscillatory behavior as shown in Fig. 1(b). The latency of each response is a random number drawn from a uniform distribution with maximum latency of one-half of the signal duration (14 time samples or 26.88 ms). Pre-stimulus noise from a human somatosensory evoked response experiment is added to represent background brain activity.

Four sets of data with SNR level ranging from −25 dB to 0 dB are generated. The SNR is defined as the ratio of the signal power to the noise power, i.e., $<x_j^2>\mathrm{tr}\{\mathbf{S}^T\mathbf{S}\}/\mathrm{tr}\{\mathbf{R}_n\}$ where $<\cdot>$ denotes an ensemble average. Figures 1(c) and 1(d) depict the simulated single-trial recordings and the corresponding averaged data for the high SNR (−10 dB) case, and Figs.1 (e) and 1(f) for the low SNR (−20 dB) case, respectively. The signal waveform is visible in the averaged data but not in the single-trial recordings.

Source localization is performed by initializing the TriViAL algorithm with estimates from the closed-form CR based ML algorithm of [12]. The signal duration is estimated from averaged data. Note that because of the variation in latency, the averaged waveform has a broadened peak (compare Fig. 1(a) and Fig. 1(d)). However, the signal duration is slightly underestimated because noise obscures the tails. The $L = 5$ temporal bases are chosen as in [13] to span 1–30 Hz frequency band. The log likelihood maps for different SNR levels are depicted in Fig. 2. At the highest SNR (0 dB), the likelihood map has a strong focal peak at the source location. The peak becomes less focal as the SNR decreases, however, the locations with the maximum value of likelihood correspond to the simulated source location for all cases.

The response parameter estimates are computed using the dipolar leadfield matrix corresponding to the location with maximum likelihood as spatial bases ($P = 2$). At each SNR we simulate amplitude and latency variation over $J = 300$ trials according to the true amplitude and latency evolutions shown in Fig. 3(b) and 3(c) (blue lines). The estimation results are shown in Fig. 3 for SNR = −20 dB. The true and estimated signal waveform shapes are depicted in Fig. 1(a) and 3(a), respectively. Although the signal duration is underestimated using the average data, the estimated waveform shape has a FWHM of 23 ms, which is slightly wider than the true FWHM. Figure 3(b) depicts the true and estimated trial amplitudes. The TriViAL algorithm is able to capture the habituation effect and the oscillatory behavior of the amplitude, although the estimates are noisy due to the low SNR. Similarly, the algorithm provides reasonable trial latency estimates as shown in Fig. 3(c) although the error is relatively large in a few trials. The numbers of iterations and computation times required for TriViAL algorithm to converge for each SNR level is shown in the first four rows of Table I. The algorithm is run using MATLAB (The MathWorks, Inc.) on a Macintosh (2.4 GHz Intel Core 2 Duo Processor, 2 GB RAM). For all SNR levels, the algorithm takes less than a minute and requires small number of iterations before convergence is reached.

In order to explore the effect of trial amplitude on the latency estimate, we arranged the latency estimates in groups of 20 according to the size of the amplitudes and computed the root-mean-square error (RMSE) for each group of $J = 20$ using

$$\mathrm{RMSE}_\tau = \sqrt{\frac{1}{J}\sum_{j=1}^{J}(\tau_j - \widehat{\tau}_j)^2}. \tag{25}$$

Figure 4 depicts the RMSE of the latency estimates as a function of the average trial amplitude for each group of 20 responses and shows that the smallest amplitude responses are associated

with the largest latency errors. The latency RMSE and normalized mean-square error (nMSE) of the amplitude estimates are depicted as a function of SNR in Fig. 5. Here the normalized mean-squared error (nMSE) of the trial amplitude is defined as

$$\mathrm{nMSE}_x = \frac{\sum_{j=1}^{J} (x_j - \bar{x}_j)^2}{\sum_{j=1}^{J} x_j^2} \tag{26}$$

The amplitude nMSE decreases more significantly than the latency RMSE as the SNR increases.

B. Real Data

Well-studied somatosensory evoked response (SER) and auditory evoked response (AER) experiments are used to validate the TriViAL algorithm. Tactile stimulation of fingers is known to evoke neural activity in the somatosensory region of the cortex. This experimental paradigm is used to verify the source localization capability of the TriViAL algorithm. An auditory experiment is employed to illustrate the effectiveness of the algorithm in estimating amplitude and latency variability. It is well established that the latency of the M100 (also known as the N1m) response peak in MEG and correspondingly the N1 response in EEG is dependent on the frequency of the auditory stimulus. In particular, the latency is larger for tones of lower frequencies [3], [10], [24]–[26]. This section demonstrates that the TriViAL algorithm is able to identify this dependence of latency on frequency.

1) SER experiment—Using a single dewar (37 channels) of the 74-channel Magness II system, two sets of MEG recordings with $J = 129$ and $J = 122$ trials are collected from a female subject whose right-hand index finger is stimulated using uniform pneumatic pressure pulses. The sampling rate is 520.8 Hz. The data is bandpass filtered at 2–40 Hz. Two bad channels are rejected, so $N = 35$. Magnetic resonance images of the subject are used to derive the 3-D cortical surface using FreeSurfer [27]. Elementary current dipoles with unknown moment orientation are placed at each node of the discretized cortical surface. Source localization is performed over the first pronounced peak in the average response waveform (approximately 80 ms after the stimulus onset at zero). The assumed signal durations and allowable ranges of the shifted response are denoted on the filtered and averaged waveforms in Fig. 6(a) and 6(b) by the red and black vertical lines, respectively. The assumed observation interval is chosen such that the maximum shift of the response peak of interest does not overlap with peaks of late components.

The log likelihood maps given by scanning the TriViAL algorithm over all dipoles on the surface are depicted in Fig. 7. The log likelihood maps for both datasets contain a focal peak near the middle of the left somatosensory cortex, consistent with our expectation.

2) AER experiment—MEG recordings from two subjects during auditory stimulation are acquired by positioning a single dewar ($N = 37$ channels) of the 74-channel Magnes II system above the left hemisphere. Pure tone bursts of 100 Hz, 250 Hz, 500 Hz, or 1 kHz frequency are presented monaurally to the subject's contralateral ear via an earphone. Each stimulus tone has a 10 ms rise and fall time with an intensity of approximately 60 dB. The intensity is adjusted to achieve roughly equal loudness between different stimulus frequencies. The frequencies of the stimuli are randomly interleaved to obtain a total of $J = 399$ trials, with each stimulus frequency occurring approximately 100 times.

We choose not to perform source localization in this example to illustrate application of the TriViAL algorithm when forward solutions are not available. Furthermore, we expect slight

shifts in cortical location for different frequency stimuli. We choose the two dominant principal components obtained from 0.5–20 Hz filtered and averaged data as our spatial bases for estimating response parameters ($P = 2$), consistent with the fact that the M100 or N1 response is often modeled by single equivalent dipole [28]. The filtered and averaged waveforms are depicted in Fig. 6(c) and 6(d) along with the assumed signal duration (red solid lines) and observation intervals (black solid lines). The assumed signal duration (171 ms or $T_s = 90$) is wider than the typical M100 response peak to account for potential differences in waveform shape associated with different stimulus frequencies. The observation interval is 250 ms or $T = 131$. We estimate the response amplitudes, response shape, and latencies by applying TriViAL to all 399 responses. We show that TriViAL is able to track the changes in latency associated with the randomized stimulus frequencies by grouping the estimated latencies based on the stimulus frequency associated with the corresponding response. Figure 8 depicts the estimated mean latency of the M100 peak for each group as a function of the stimulus frequency. The error bars denote the standard error of the mean. Decrease in the mean M100 latency in the range of 12–25 ms between lowest and highest stimulus frequency is clearly observed in both subjects as the stimulus frequency increases. These results are consistent with previously reported latency prolongation obtained by separately presenting each stimulus frequency [3], [10], [28]. The corresponding signal waveform shape estimates are depicted in Fig. 9. The last two rows of Table I displays the required number of iterations and computation time for convergence of the algorithm when applied to the two AER data sets. Similar to the simulated data example, the algorithm converges in less than ten iterations in approximately two minutes.

The impact of jointly estimating amplitude and latency on amplitude estimates is illustrated in Fig. 10 by comparing histograms of the estimated amplitudes using the TriViAL algorithm to the amplitude-only algorithm of [11]. The amplitude-only algorithm results in negative estimated amplitudes in 9.27 percent of the responses, while the TriViAL algorithm results only in positive amplitude estimates. Negative amplitude estimates are not physically meaningful since they imply reversal of cortical current flow.

VI. DISCUSSION

The CR spatio-temporal framework for evoked response data has been used successfully in MEG/EEG applications in the past [12]–[14], but is unable to track variability of individual evoked responses. The TriViAL algorithm presented in this paper extends the spatio-temporal evoked response framework to estimate amplitudes and latencies of individual evoked responses. Spatial and temporal bases are employed to provide a low-dimensional representation for the aspect of the evoked response that is consistent across trials while explicitly modeling amplitude and latency parameters. This spatio-temporal framework results in improved discrimination between signal and noise, provided the evoked response is well-described by the spatio-temporal bases, and consequently results in improved quality waveform, amplitude, and latency estimates. Furthermore, the use of spatial bases endows our approach with source localization capability. The TriViAL algorithm is effective at source localization as well as waveform, amplitude, and latency estimation for the SNRs typical of evoked response data.

The framework proposed in this paper assumes that the responses lie in a spatio-temporal space defined by the spatial and temporal bases, with constant waveform shape and only the amplitude and latency changing from trial to trial. All response components that satisfy these signal characteristics are modeled, whereas all other response components are included in the estimated spatial covariance matrix of the noise. Note that in the CR approach all variable response components are included in the noise. Maximum likelihood provides a principled means for estimating the unknown response parameters, and the TriViAL algorithm developed

here are simple to implement and guaranteed to converge to a local maximum of the likelihood function.

Explicit modeling of response latency results in significant improvements in waveform shape and response amplitude estimation. Ignoring modest latency variations can result in obscuring of multiple peaks in the response due to temporal smoothing, while ignoring larger variations in latency can result in false peaks in the signal waveform. Modeling latency also improves estimation of response amplitude since it prevents the amplitude estimates from attempting to compensate for mismatch in response shape. We have shown that modeling latency greatly reduces the occurrence of non-physical, negative amplitude estimates.

The limitations of existing approaches for assessing amplitude and latency variability are discussed in detail in [11]. In summary, existing methods either: apply to single channel measurements or are not formulated in terms of cortical source space [9], [17]; use suboptimal two-step approaches where the cortical source space problem is treated separately from amplitude and/or latency estimation [29], [30]; or require estimation of a large number of unknown parameters [18]. In contrast, the TriViAL algorithm utilizes spatial bases to relate the measured sensor data back to the original source space on the cortex and simultaneously estimates the optimum signal waveform parameters, noise covariance matrix, amplitude, and latency using the ML principle. The TriViAL algorithm estimates latency by cross-correlating the current spatially whitened waveform shape estimate with spatially whitened data, analogous to heuristic cross-correlation approaches [15], [31]. However, use of appropriate spatial and temporal bases mitigates the unrealistic waveform sharpening that can result from the Woody filter [15].

Performance of the TriViAL algorithm in source localization and response estimation is demonstrated with both simulated and measured somatosensory and auditory MEG data in a realistic SNR range. The algorithm performs reasonably well when the SNR is sufficiently large. As expected, the resolution of the localization result as well as the quality of the response waveform, trial amplitudes, and trial latency estimates decrease as SNR decreases.We observe that the trial amplitude estimation error decreases more significantly than the trial latency estimation error when the SNR increases. We also observe that the RMSE of the latency estimates depends on the amplitude of the corresponding trials. In particular, for a given SNR the latency error is generally greater for trials with relatively weak amplitude.

The ECM algorithm is only guaranteed to find a local maximum of the likelihood surface. An approach often used to avoid local maxima with ECM algorithms is to perform estimation multiple times with randomized initial conditions on the parameters and choose the set of parameters producing the highest likelihood. It is not necessary to employ this so-called multistart approach to produce the strong results presented in this paper. An expected range of latencies is known for many experimental paradigms and can be used to limit the search range. In our experience the choice of response duration does not have much effect on estimation performance provided it is sufficiently long to capture the dominant features in the response. Increasing the observation interval generally increase computation time due to the increased latency search space. Criteria for choosing the response duration and observation interval are likely to vary with the application.

The effectiveness of the TriViAL algorithm for latency estimation is demonstrated using the well-known dependence of the M100 response latency in MEG (N1 response in EEG) on the frequency of auditory stimuli. The latency increases as stimulus frequency decreases below 1 kHz [3], [10], [24], [28], suggesting that stimulus attributes may be reflected in evoked response latency variations [28], [32]. This phenomenon represents an ideal paradigm for evaluating latency estimation methods. We present a series of tones with pseudo-randomly chosen

stimulus frequencies and estimate the latencies of each response using the TriViAL algorithm with no prior knowledge of the stimulus frequency. The estimated mean latencies associated with each stimulus frequency reproduce the known relationship between latency and stimulus frequency with excellent agreement between both subjects studied. Furthermore, the standard error of the mean is small and supports the frequency dependence of the latency estimates. This result provides compelling evidence of the efficacy of the TriViAL algorithm.

It is possible in principle to extend the TriViAL algorithm to a model containing multiple independent components, each having independent amplitudes, latencies, and spatio-temporal response shapes. This would require a multiple dimensional search to estimate latency parameters and thus would be limited to relatively small numbers of components. The challenge with such an extension is to obtain data with sufficiently high SNR to enable reliable estimation of all unknown model parameters.

Acknowledgments

This work was supported in part by the National Institutes of Health (NIH) under Grant R21EB005473.

REFERENCES

1. Wastell D, Kleinman D. Potentiation of the habituation of human brain potentials. Biological Psychology 1980;vol. 10:21–29. [PubMed: 7407281]
2. Arieli A, Sterkin A, Grinvald A, Aertsen A. Dynamics of ongoing activity: explanation of the large variability in evoked cortical responses. Science 1996;vol. 273(no. 5283):1868–1871. [PubMed: 8791593]
3. Roberts T, Poeppel D. Latency of auditory evoked M100 as a function of tone frequency. NeuroReport 1996;vol. 7:1138–1140. [PubMed: 8817518]
4. Truccolo W, Ding M, Knuth K, Nakamura R, Bressler S. Trialto-trial variability of cortical evoked responses: implications for the analysis of functional connectivity. Clinical Neurophysiology 2002;vol. 113:206–226. [PubMed: 11856626]
5. Pantev C, Hoke M, Lehnertz K, Lütkenhöner B, Anogianakis G, Wittkowski W. Tonotopic organization of the human auditory cortex revealed by transient auditory evoked magnetic fields. Electroenceph. Clin. Neurophysiol 1988;vol. 69:160–170. [PubMed: 2446835]
6. Thornton ARD, Harmer M, Lavoie B. Selective attention increases the temporal precision of the auditory n100 event-related potential. Hearing Research 2007;vol. 230:73–79. [PubMed: 17606341]
7. Kisley M, Gerstein G. Trial-to-trial variability and state-dependent modulation of auditory-evoked responses in cortex. Journal of Neuroscience 1999;vol. 19(no. 23):10 451–10 460.
8. Ioannides A. Magnetoencephalography as a research tool in neuroscience: state of the art. The Neuroscientist 2006;vol. 12(no. 6):524–544. [PubMed: 17079518]
9. Jaśkowski P, Verleger R. Amplitudes and latencies of single-trial ERP's estimated by a maximum-likelihood method. IEEE Trans. Biomed. Eng 1999;vol. 46(no. 8):987–993.
10. Salajegheh A, Link A, Elster C, Burghoff M, Sander T, Trahms L, Poeppel D. Systematic latency variation of the auditory evoked M100: from average to single-trial data. NeuroImage 2004;vol. 23:288–295. [PubMed: 15325376]
11. Limpiti T, Van Veen B, Attias H, Nagarajan S. A spatiotemporal framework for estimating trial-to-trial amplitude variation in event-related MEG/EEG. IEEE Trans. Biomed. Eng 2009;vol. 56(no. 3): 633–645. [PubMed: 19272883]
12. Dogandžić A, Nehorai A. Estimating evoked dipole responses in unknown spatially correlated noise with EEG/MEG arrays. IEEE Trans Signal Processing 2000;vol. 48(no. 1):13–25.
13. Baryshnikov B, Van Veen B, Wakai R. Maximum-likelihood estimation of low-rank signals for multiepoch MEG/EEG analysis. IEEE Trans Biomed. Eng 2004;vol. 51(no. 11):1981–1993. [PubMed: 15536900]
14. Limpiti T, Van Veen B, Wakai R. Cortical patch basis model for spatially extended neural activity. IEEE Trans. Biomed. Eng 2006;vol. 53(no. 9):1740–1754. [PubMed: 16941830]

15. Woody C. Characterization of an adaptive filter for the analysis of variable latency neuroelectric signals. Medical and Biological Engineering 1967;vol. 5:539–554.

16. McFarland D, Cacace A. Separating stimulus-locked and unlocked components of the auditory event-related potential. Hearing Research 2004;vol. 193:111–120. [PubMed: 15219326]

17. Tuan P, Möcks J, Kohler W, Gasser T. Variable latencies of noisy signals: estimation and testing in brain potential data. Biometrika 1987;vol. 74(no. 3):525–533.

18. de Munck J, Bijma F, Gaura P, Sieluzycki C, Branco M, Heethaar R. A maximum-likelihood estimator for trial-to-trial variations in noisy MEG/EEG data sets. IEEE Trans. Biomed. Eng 2004;vol. 51(no. 12):2123–2128. [PubMed: 15605859]

19. Scherg M, von Cramon D. Two bilateral sources of the late AEP as identified by a spatio-temporal dipole model. Electroenceph. Clin. Neurophysiol 1985;vol. 62:32–44. [PubMed: 2578376]

20. Mosher, J.; Leahy, R.; Shattuck, D.; Baillet, S. MEG source imaging using multipolar expansions; Proc. 16th Conf. Inf. Process. Med. Imag. 891 (IPMI 1999); Visegrád, Hungary: Springer-Verlag; 1999 Jun. p. 15-28.

21. Nolte G, Curio G. Current multipole expansion to estimate lateral extent of neuronal activity: a theoretical analysis. IEEE Trans Biomed. Eng 2000;vol. 47(no. 10):1347–1355. [PubMed: 11059169]

22. Meng X, Rubin D. Maximum likelihood estimation via the ECM algorithm: a general framework. Biometrika 1993;vol. 80(no. 2):267–278.

23. Scharf, L. Statistical signal processing: detection, estimation, and time series analysis. Reading, Massachusetts: Addison-Wesley; 1990.

24. Jacobson G, Lombardi D, Gibbens N, Ahmad B, Newman C. The effects of stimulus frequency and recording site on the amplitude and latency of multichannel cortical auditory evoked potential (CAEP) component N1. Ear and Hearing 1992;vol. 13:300–306. [PubMed: 1487089]

25. Verkindt C, Bertrand O, Perrin F, Echallier J, Pernier J. Tonotopic organization of the human auditory cortex: N100 topography and multiple dipole model analysis. Electroenceph. Clin. Neurophysiol 1995;vol. 96:143–156. [PubMed: 7535220]

26. Woods D, Alain C, Covarrubias D, Zaidel O. Frequency-related differences in the speed of human auditory processing. Hearing Research 1993;vol. 66:46–52. [PubMed: 8473245]

27. Dale A, Fischl B, Sereno M. Cortical surface-based analysis i: Segmentation and surface reconstruction. NeuroImage 1999;vol. 9(no. 2):179–194. [PubMed: 9931268]

28. Roberts T, Ferrari P, Stufflebeam S, Poeppel D. Latency of the auditory evoked neuromagnetic field components: stimulus dependence and insights toward perception. Journal of Clinical Neurophysiology 2000;vol. 17:114–129. [PubMed: 10831104]

29. Spreckelsen M, Bromm B. Estimation of single-evoked cerebral potentials by means of parametric modeling and Kalman filtering. IEEE Trans Biomed. Eng 1988;vol. 35(no. 9):691–700.

30. Lange D, Pratt H, Inbar G. Modeling and estimation of single evoked brain potential components. IEEE Trans. Biomed. Eng 1997;vol. 44(no. 9):791–799. [PubMed: 9282471]

31. Thornton ARD. Evaluation of a technique to measure latency jitter in event-related potentials. J. of Neuroscience Methods 2008;vol. 168:248–255.

32. Forss N, Mäkelä JP, McEvoy L, Hari R. Temporal integration and oscillatory responses of the human auditory cortex revealed by evoked magnetic fields to click trains. Hearing Research 1993;vol. 68:89–96. [PubMed: 8376218]

Biographies

Tulaya Limpiti (S’02-M’08) received the B.S. degree (with highest honors) from Northwestern University, Evanston, IL in 2002 and the M.S. and Ph.D. degrees from the University of Wisconsin–Madison, Madison, WI in 2004 and 2008, respectively, all in electrical engineering.

She received the University of Wisconsin Graduate School Fellowship for 2002-03 and College of Engineering Grainger Distinguished Graduate Fellowship for 2003-05 while working on the Ph.D. degree.

In 2008 she was a postdoctoral researcher at the University of Wisconsin– Madison. Currently, she is a lecturer at the Faculty of Engineering, King Mongkut's Institute of Technology Ladkrabang, Thailand. Her research interests include statistical and array signal processing, with emphasis on algorithm development and analysis for biomedical applications.

Barry D. Van Veen (S'81-M'86-SM'97-F'02) was born in Green Bay, WI. He received the B.S. degree from Michigan Technological University in 1983 and the Ph.D. degree from the University of Colorado in 1986, both in electrical engineering. He was an ONR Fellow while working on the Ph.D. degree.

In the spring of 1987 he was with the Department of Electrical and Computer Engineering at the University of Colorado-Boulder. Since August of 1987 he has been with the Department of Electrical and Computer Engineering at the University of Wisconsin-Madison and currently holds the rank of Professor. His research interests include signal processing for sensor arrays and biomedical applications of signal processing.

Dr. Van Veen was a recipient of a 1989 Presidential Young Investigator Award from the National Science Foundation and a 1990 IEEE Signal Processing Society Paper Award. He served as an associate editor for the IEEE Transactions on Signal Processing and on the IEEE Signal Processing Society's Statistical Signal and Array Processing Technical Committee and the Sensor Array and Multichannel Technical Committee. He is a Fellow of the IEEE and received the Holdridge Teaching Excellence Award from the ECE Department at the University of Wisconsin in 1997. He coauthored "Signals and Systems," (1st Ed. 1999, 2nd Ed., 2003 Wiley) with Simon Haykin.

Ronald T. Wakai was born in East Orange, NJ, in 1958. He received the B.A. degree with honors in physics from Cornell University, Ithaca, NY, in 1980 and the Ph.D. degree in physics from the University of Illinois, Urbana, in 1987.

Since then, he has been with the Department of Medical Physics at the University of Wisconsin, Madison, WI, where he is currently a Professor. His research interests include basic and technical aspects of fetal biomagnetism and adult MEG.

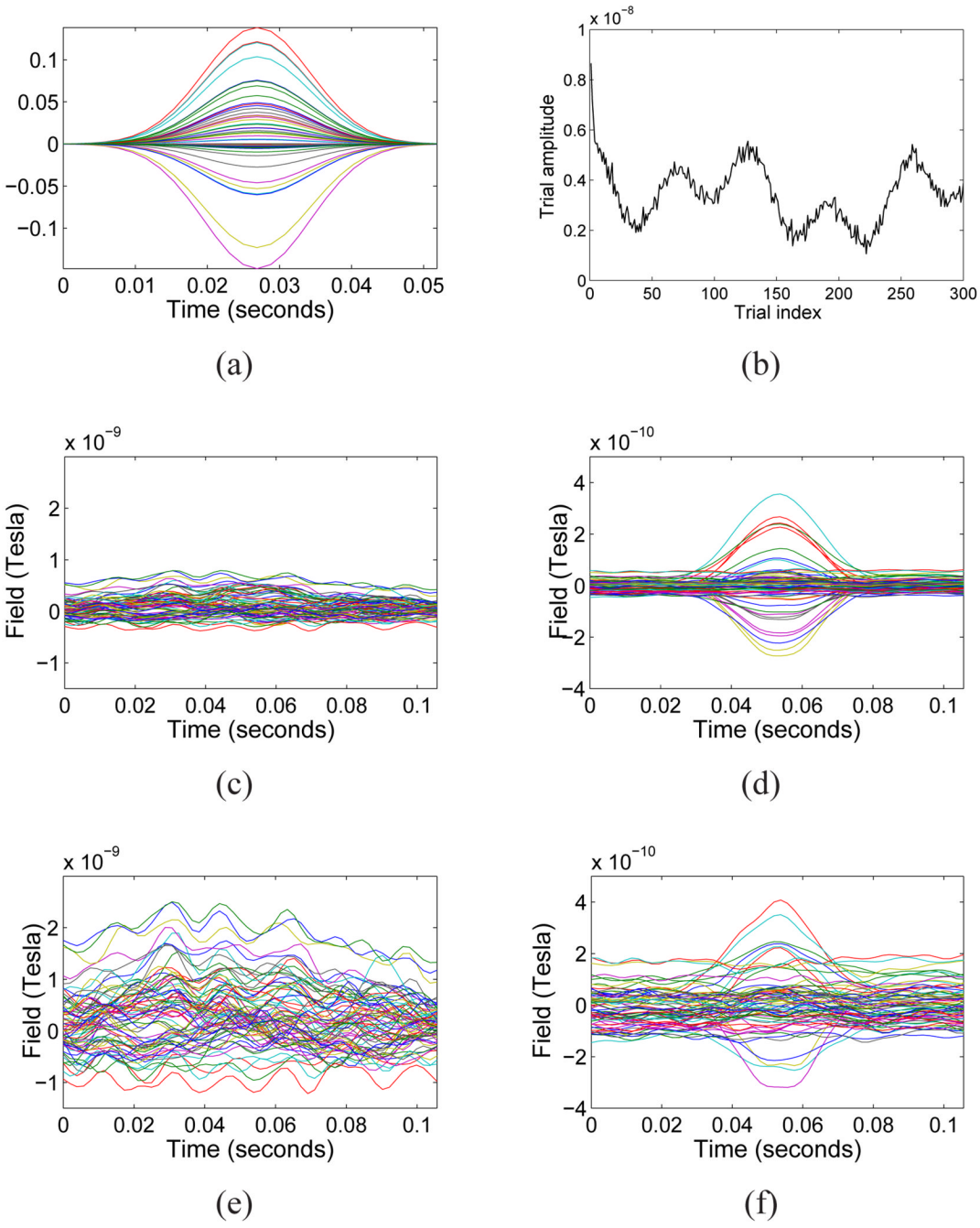

Fig. 1.

Example of simulated recordings. (a) Signal waveform. (b) Simulated response amplitudes. (c) Single-trial at SNR = −10 dB. (d) Average over 300 trials at SNR = −10 dB. (e) Single-trial at SNR = −20 dB. (f) Average over 300 trials at SNR = −20 dB.

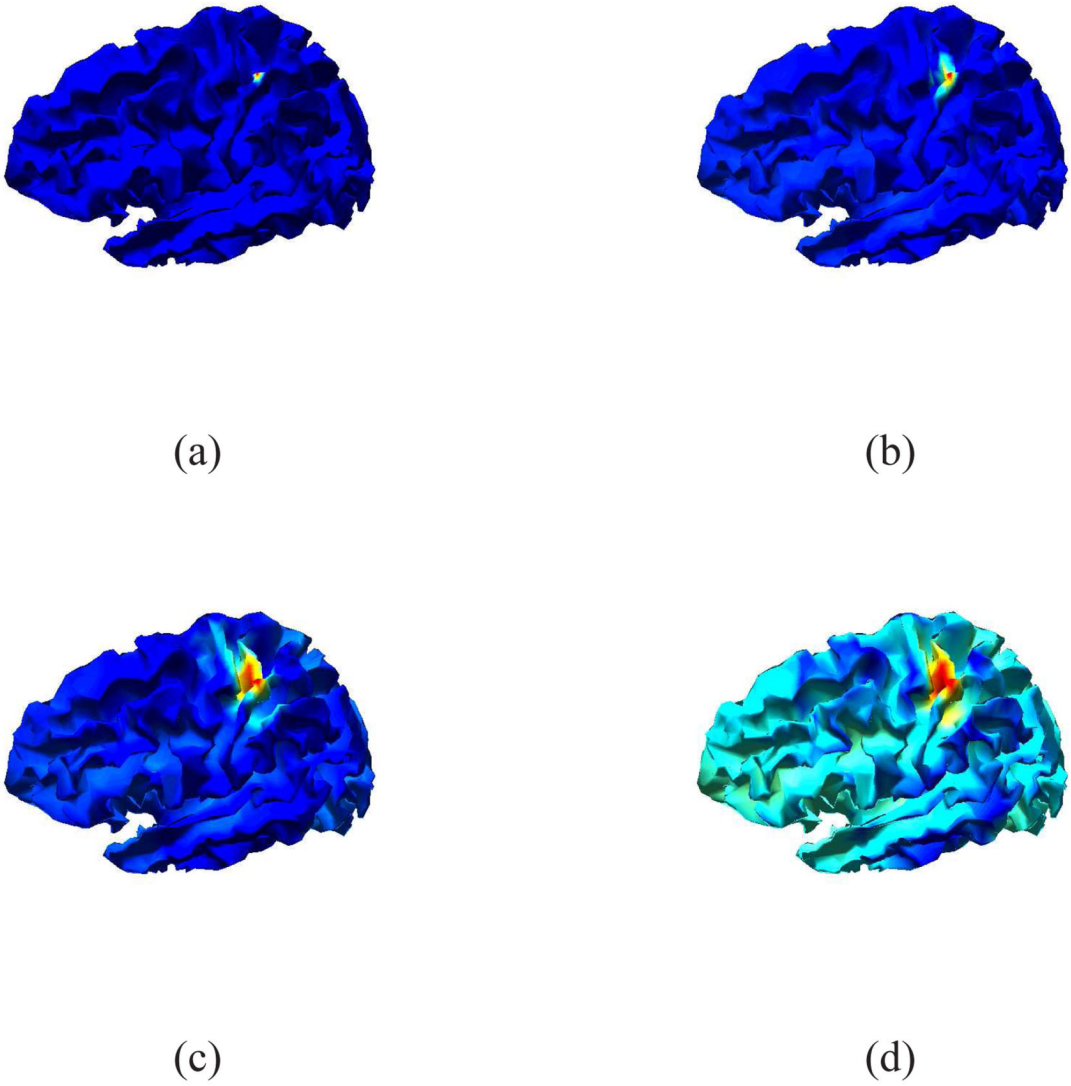

Fig. 2.
Log likelihood maps for simulated data example. (a) SNR = 0 dB. (b) SNR = −10 dB. (c) SNR = −20 dB. (d) SNR = −25 dB.

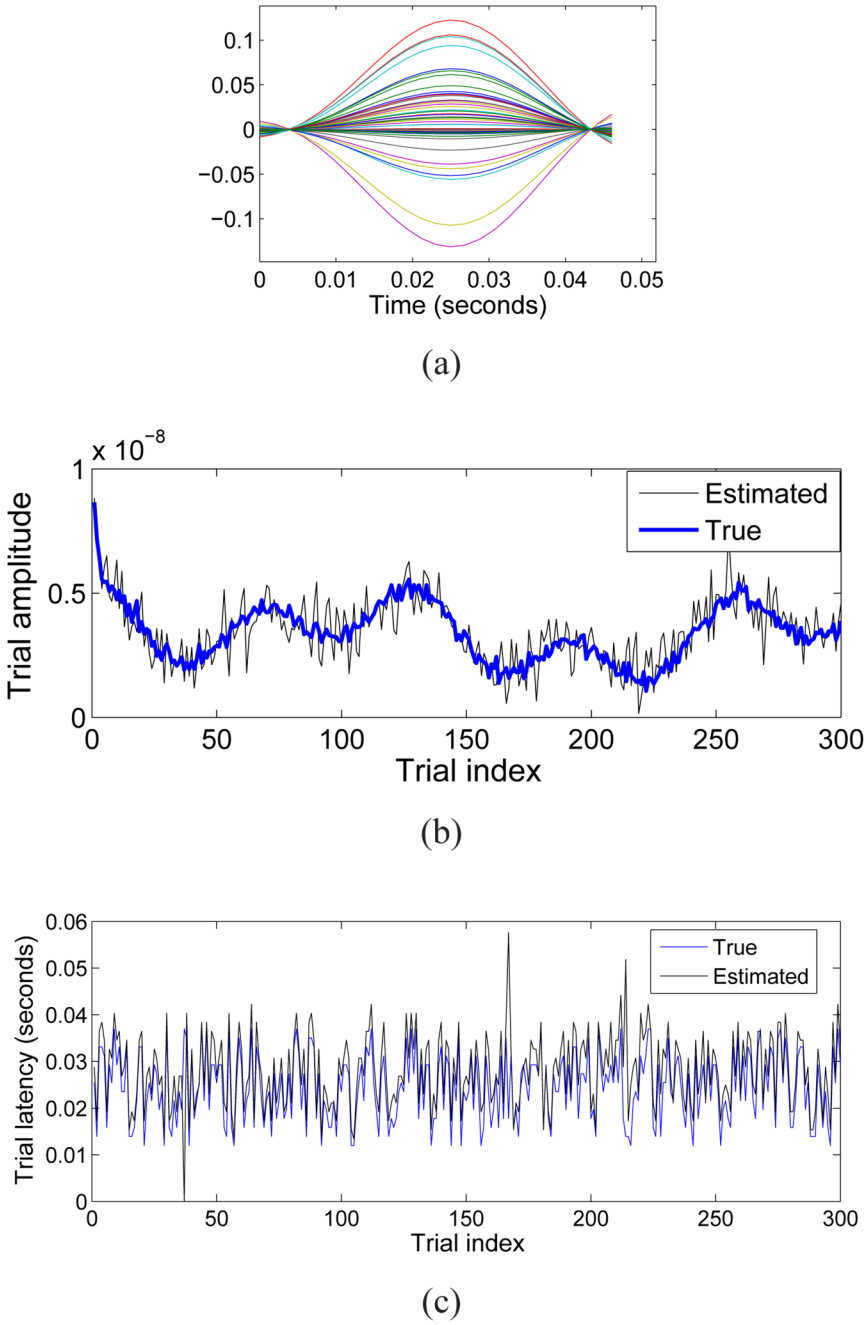

Fig. 3.

Color plots of estimated signal waveform shape, amplitudes, and latencies for simulated data with SNR = −20 dB. (a) Estimated waveform shape. (b)True (blue) and estimated (black) trial amplitudes. (c) True (blue) and estimated (black) trial latencies.

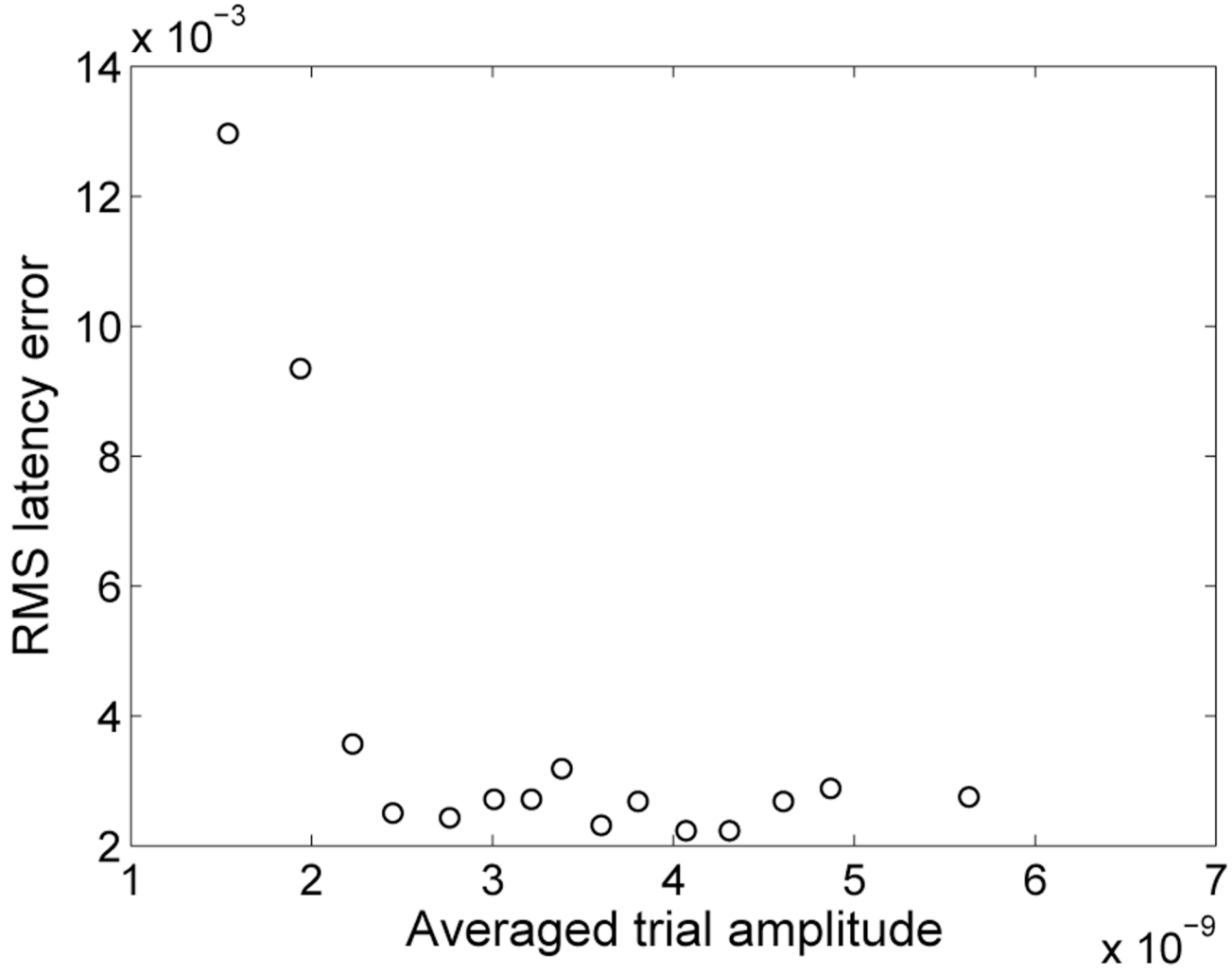

Fig. 4.
RMS latency error as a function of average trial amplitude over groups of 20 trials sorted according to amplitude.

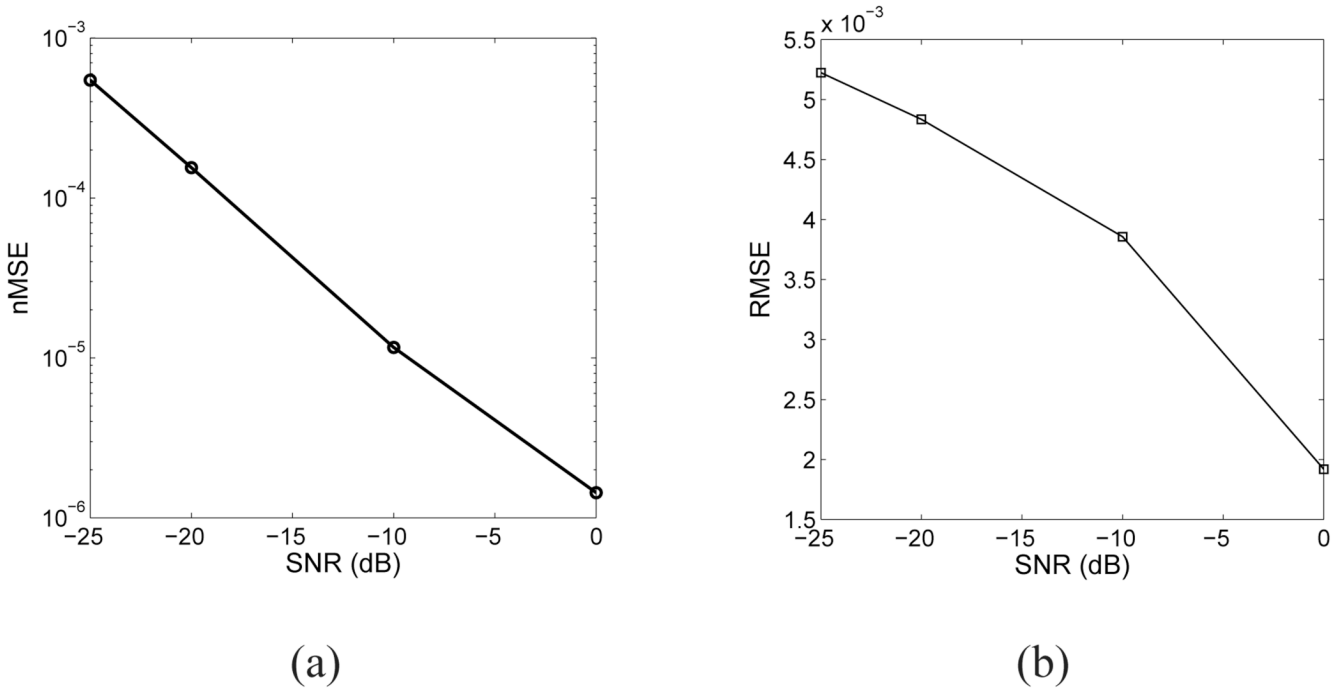

Fig. 5.
Errors of the estimated trial amplitude and latency as a function of SNR. (a) Normalized mean squared error (nMSE) of amplitude on a log scale. (b) Root mean squared error (RMSE) of latency on a linear scale.

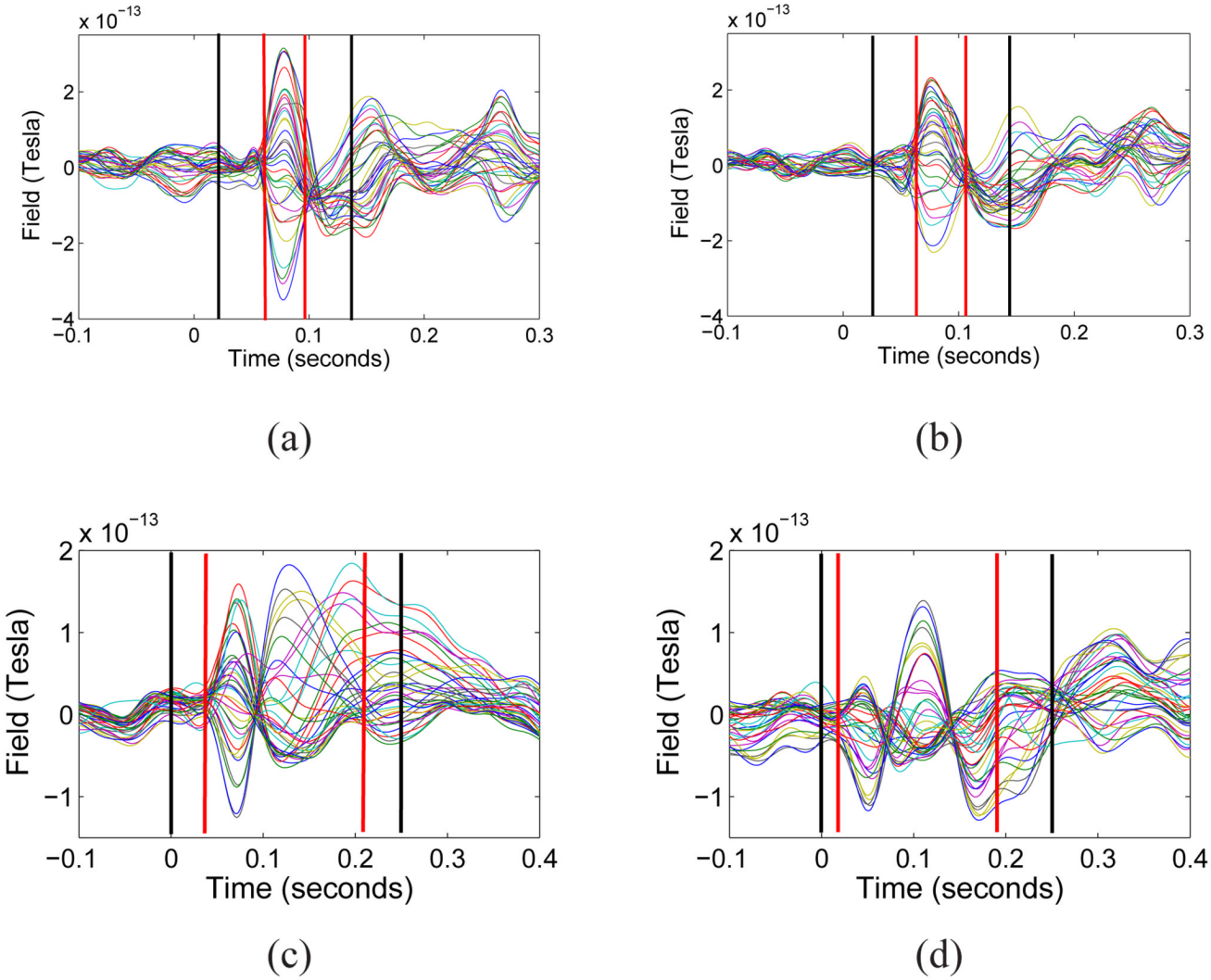

Fig. 6.
Filtered and averaged evoked response data. Red vertical lines denote the assumed response duration (T_s) while the black vertical lines denote the assumed observation interval (T). (a–b) Two SER experiments. (c–d) Two AER experiments.

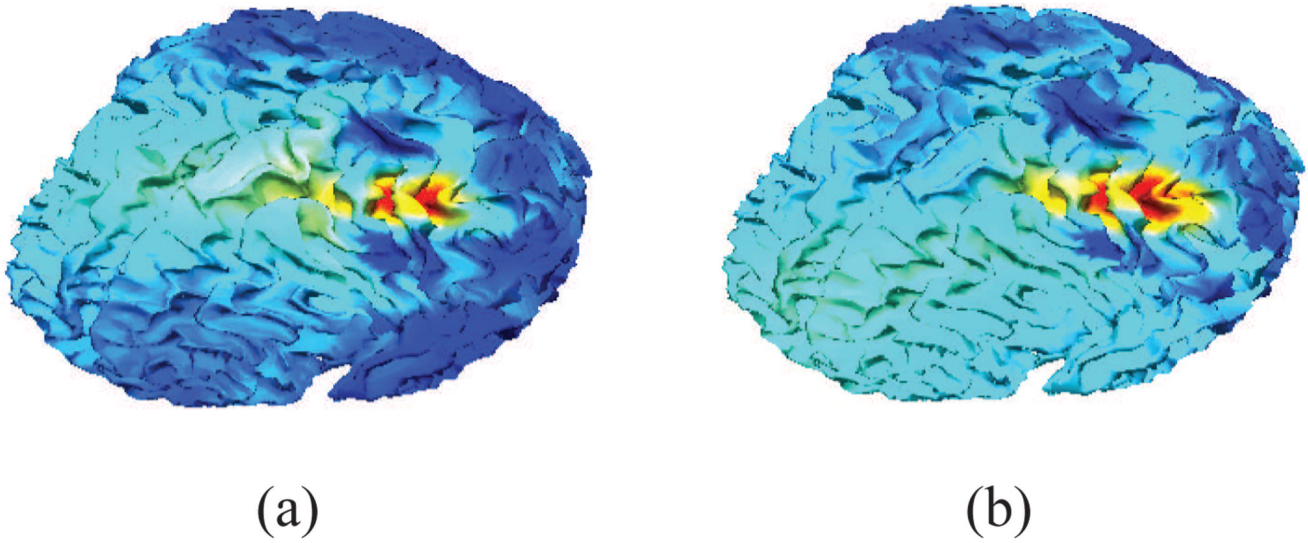

Fig. 7.
Log likelihood maps for the SER experiment. (a) First dataset. (b) Second dataset.

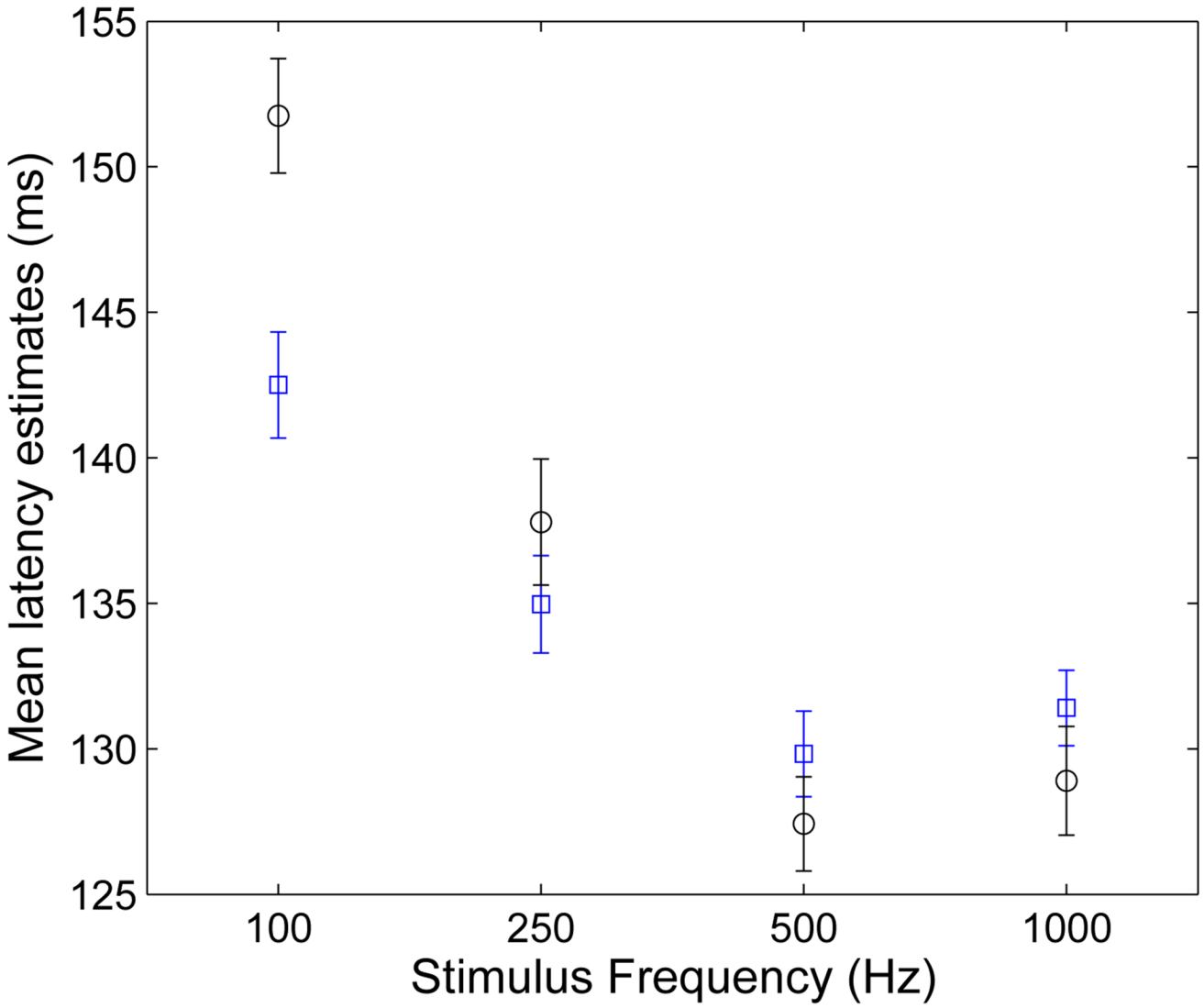

Fig. 8.
Estimated trial latency for the AER experiment (mean + standard error of the mean over trials). Black circle: First subject; Blue square: Second subject.

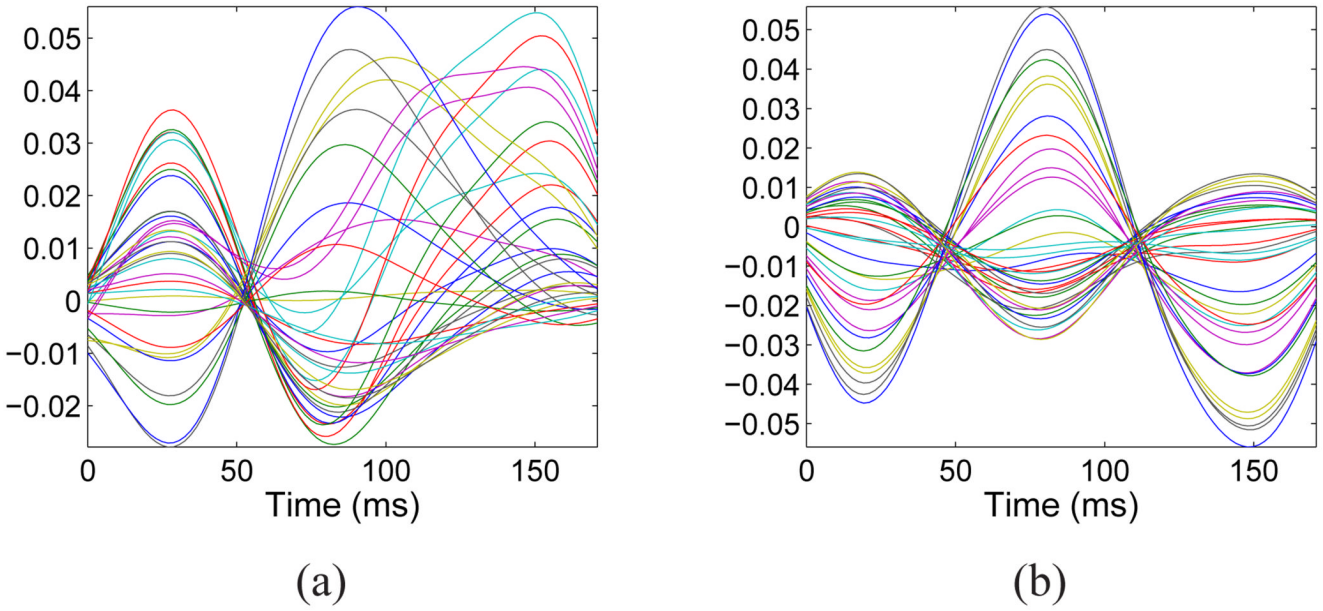

Fig. 9.
Signal waveform shape estimates for the AER experiment. (a) First subject. (b) Second subject.

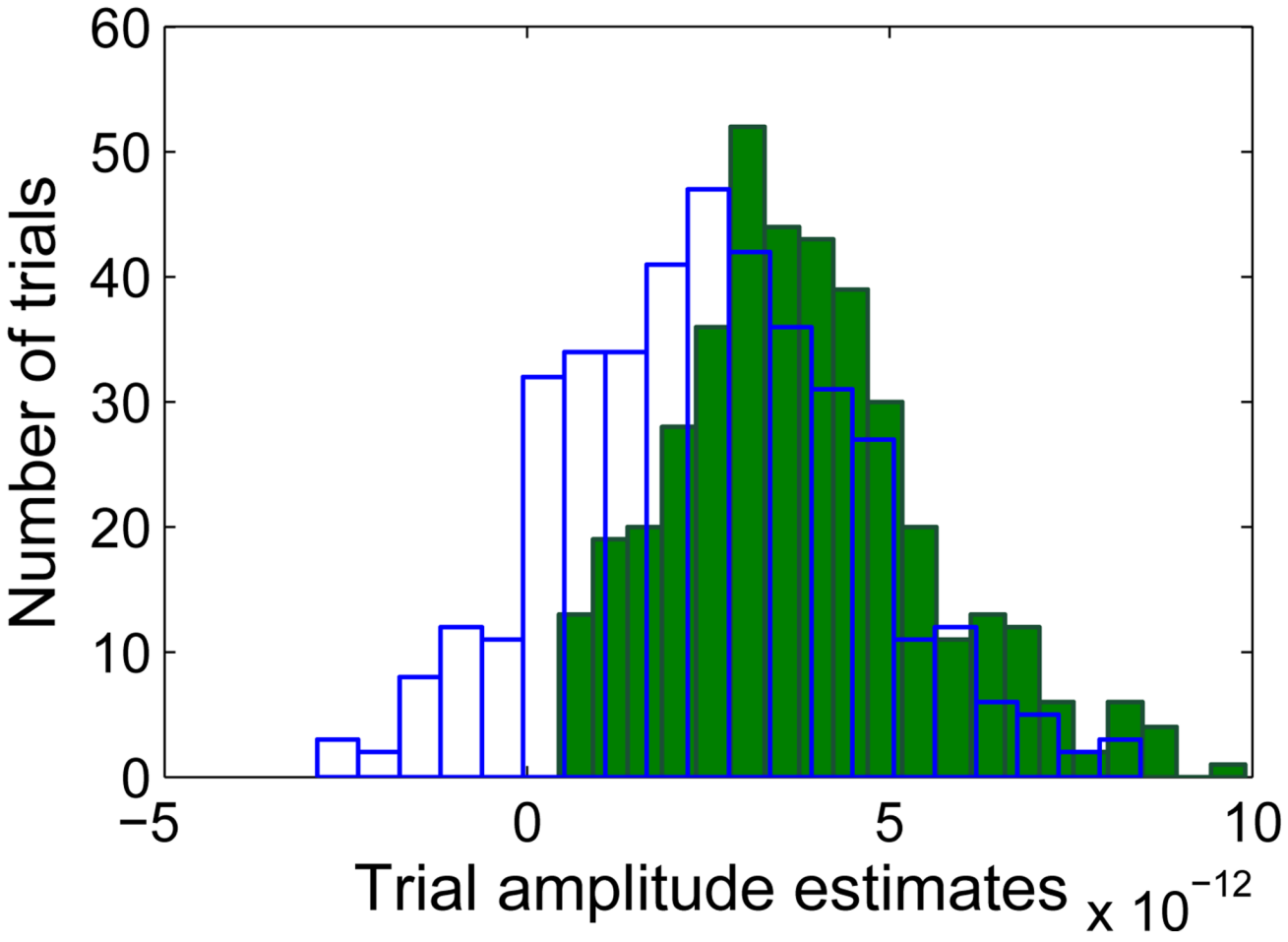

Fig. 10.
Histograms of the estimated trial amplitudes using TriViAL algorithm (green) and algorithm in [11] (blue).

TABLE I

Required number of iteration and computation time for response parameter estimation

		Number of iterations	CPU time (s)
Simulated data:	SNR = 0 dB	8	46.9
	SNR = −10 dB	8	50.1
	SNR = −20 dB	6	31.6
	SNR = −25 dB	7	45.4
Real AER data:	first subject	6	109.5
	second subject	10	120.4